

SLIMM DECAY HEAT REMOVAL BY NATURAL CIRCULATION OF AMBIENT AIR

Luis Palomino^{1,2}, Mohamed S. El-Genk^{1,2,3,4,*}

¹The Institute for Space and Nuclear Power Studies, ²Nuclear Engineering Department, ³Mechanical Engineering Department, ⁴Chemical and Biological Engineering Department
University of New Mexico, Albuquerque, NM, 87131, USA

ABSTRACT

This paper presents the results of 3-D Computational Fluid Dynamic (CFD) and thermal-hydraulic analyses investigating passive decay heat removal for the Scalable Liquid Metal cooled small Modular (SLIMM) reactor by natural circulation of ambient air, in case of a malfunction of the in-vessel helically coiled tubes, Na/Na heat exchanger. Results show that the longitudinal metal fins along the outer surface of the reactor guard vessel effectively increase the heat removal by air natural circulation. The thermal radiation from the guard vessel outer wall and metal fins is a major contributor to the heat removal of the decay heat by ambient air, accounting for 29%-42% of the total rate of heat removal. Results showed that the decay heat removal by ambient air is quite effective, even without metal fins along the outer surface of the guard vessel wall (~ 1.0 MW_{th}). The metal fins increase the rate of the heat removal by naturally convection of ambient air by an additional 26% to 1.26 MW_{th}. Without metal fins along the outer surface of the guard vessel wall, the average temperature of the circulating liquid sodium in the reactor primary vessel peaks at ~ 821.7 K, ~ 1.5 hr after reactor shutdown and decreases to 400 K ~ 22.2 hr after reactor shutdown. With metal fins, the higher rate of heat removal (1.26 MW_{th}), limits the peak temperature of the in-vessel liquid sodium to ~ 806 K, only ~ 40 minutes (or 0.665 hr) after reactor shutdown. These results confirm a large safety margin, > 330 K, from the boiling temperature of liquid sodium (~ 1156 K at 0.1 MPa).

KEYWORDS

SLIMM-Small modular reactor, natural circulation of ambient air, Computational Fluid Dynamics (CFD), thermal-hydraulics, passive decay heat removal, liquid sodium

1. INTRODUCTION

The Scalable Liquid Metal cooled small Modular (SLIMM) reactor is developed at the University of New Mexico's Institute for Space and Nuclear Power Studies, to generate 10-100 MW_{th} for extend periods without refueling. It operates fully passive, except for the in-vessel drives for the reactor control and emergency shutdown [1-3]. With the aid of an in-vessel chimney and a heat exchanger (HEX), comprised of concentric helical coils at the top of the downcomer, natural circulation of in-vessel liquid sodium passively cools the reactor core during nominal operation and after shutdown (Fig. 1). The SLIMM reactor is to be fabricated, assembled and sealed at the factory, and shipped to the construction site by rail, a truck or a barge. The reactor would be installed below ground to avoid direct impact by missiles or aircraft, and mounted on seismic oscillation bearings, to resist earthquakes.

With the same core design, the reactor thermal power increases with increasing the heights of the in-vessel chimney and the helically coiled tubes HEX (Fig. 1). For a fixed core inlet temperature of 610 K,

* Corresponding Author: mgenk@unm.edu, (505) 277-5442

the flow rate and temperature of the liquid sodium exiting the core increase with increasing the reactor thermal power and/or the height of the in-vessel chimney [1, 3, 4]. This is done while ascertaining that the sodium exit temperature from the core remains < 820 K, depending on the reactor power and the chimney height (Fig. 1). At these core inlet and exit temperatures, corrosion of the HT-9 stainless steel of the UN fuel rods cladding, the core structure and the reactor primary and guard vessels is negligible [5-7].

Figure 1, presents a longitudinal cross-section view of the SLIMM reactor, including the core, the in-vessel chimney and HEX, the reactor primary and guard vessels, the in-vessel control drives and the core support structure. The HT-9 steel primary and guard vessels of the SLIMM reactor are made of two sections. The lower section houses the reactor core, and the core control drives and the upper section houses the chimney (≤ 8 m tall) and the helically coiled tubes Na/Na HEX. The heights of the in-vessel chimney and HEX, and hence that of the upper section of the primary and guard vessels, increase with increasing the reactor thermal power.

The primary and guard vessels (Figs 1 and 2), with walls that are only a few inches thick, are each capable of containing the reactor core, and the in-vessel liquid sodium, HEX and other core structure and components. The total mass of the in-vessel liquid sodium increases from 18 MT to 38 MT with increasing the chimney height, H_{Ch} , from 2 m to 8 m (Fig. 1) [1, 3].

The difference between the static pressure heads in the downcomer and that in the core and the chimney drives the in-vessel natural circulation of the liquid sodium. The circulation path traverses the reactor core, the chimney, the upper plenum, the HEX, the downcomer, and the lower plenum (Fig. 1) through the core [3, 4]. The circulating liquid sodium through the reactor's primary vessel removes and transports the heat generated in the core by fission during nominal operation or by radioactive decay after reactor shutdown, to the HEX. The placement of the HEX at the top of the downcomer maximizes the driving static heat for natural circulation (Fig. 1). The cooler sodium exiting the HEX flows through the downcomer to the lower plenum, before entering the core at 610 K (Fig. 4). The lower temperature and vapor pressure of the liquid sodium exiting the core during nominal operation (≤ 820 K and 1.6 kPa) provide large operation and safety margin to the boiling point (~ 1156 K and 0.1 MPa) [8].

During nominal reactor operation, argon gas fills the small gap between the HT-9 steel primary and guard vessels (Figs. 1 and 2), which together with the highly reflective surfaces of the facing walls, reduce the heat losses from the primary vessel during nominal reactor operation (Figs. 1 and 2). In case of a malfunction of the in-vessel HEX, liquid sodium replaces the argon gas in the gap. This increases the thermal conductance of the gap for removing the decay heat from the circulating liquid sodium through the downcomer of reactor primary vessel. Natural circulation of in-vessel liquid sodium removes the decay heat generated in the core to the primary vessel wall in the downcomer (Fig. 1). The heat transfers by convection to the inner surface of the primary vessel wall and by conduction through the wall, the sodium gap, and the wall of the guard vessel to the surface exposed to ambient airflow in the hot riser. Natural convection of the ambient air removes the heat dissipated at the outer surface of guard vessel (Fig. 2). The difference between the static pressure heads of the ambient air intake duct and the hot air

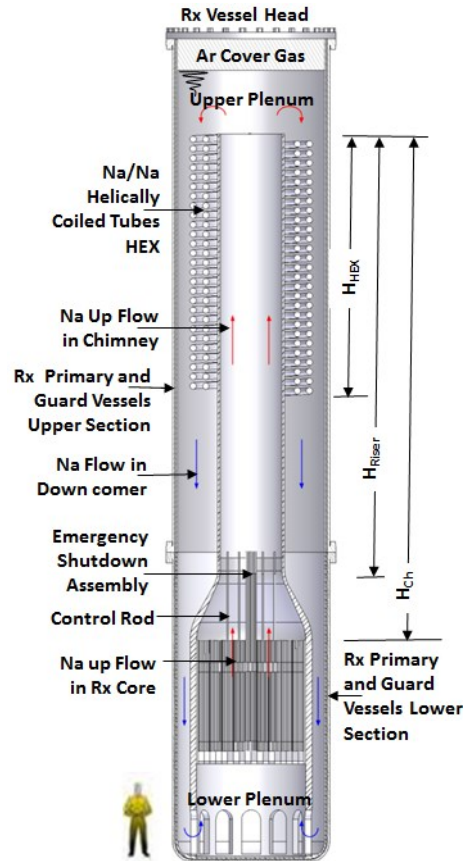


Figure 1. A Longitudinal Cross-Sectional of the SLIMM Reactor with an 8 m Tall Chimney [1-3].

riser, along the outer surface of the guard vessel, passively drives the airflow for removing the decay heat by natural convection of ambient air.

The tall and annular hot air riser and the cold air intake ducts are separated by a concrete wall (Figs 2 and 3), with a thin steel liner on the hot side and a thermal insulation on the cold side. Owing to the high temperature of the liquid sodium in the primary vessel after reactor shutdown, thermal radiation from the guard vessel outer surface is a contributor to the removal of the heat dissipated at the outer surface of the guard vessel wall. The height of the vessel, which depends on the height of the in-vessel chimney, also affects the heat removal rate from the outer surface of the guard vessel. The metal (Copper) fins could extend vertically beyond the height of the reactor vessel to enhance the heat removal by ambient air. The metal fins along the outer surface of the guard vessel wall increase the surface area for heat removal by the air natural convection and thermal radiation to the facing steel liner, and then by convection to the flowing air in the hot riser duct (Fig. 2). In addition, the liquid metal (LM) heat pipes along the base of the extended metal fins serve as heat spreaders for enhancing axial conduction and improving the heat removal from the outer surface of the guard vessel wall (Fig. 2).

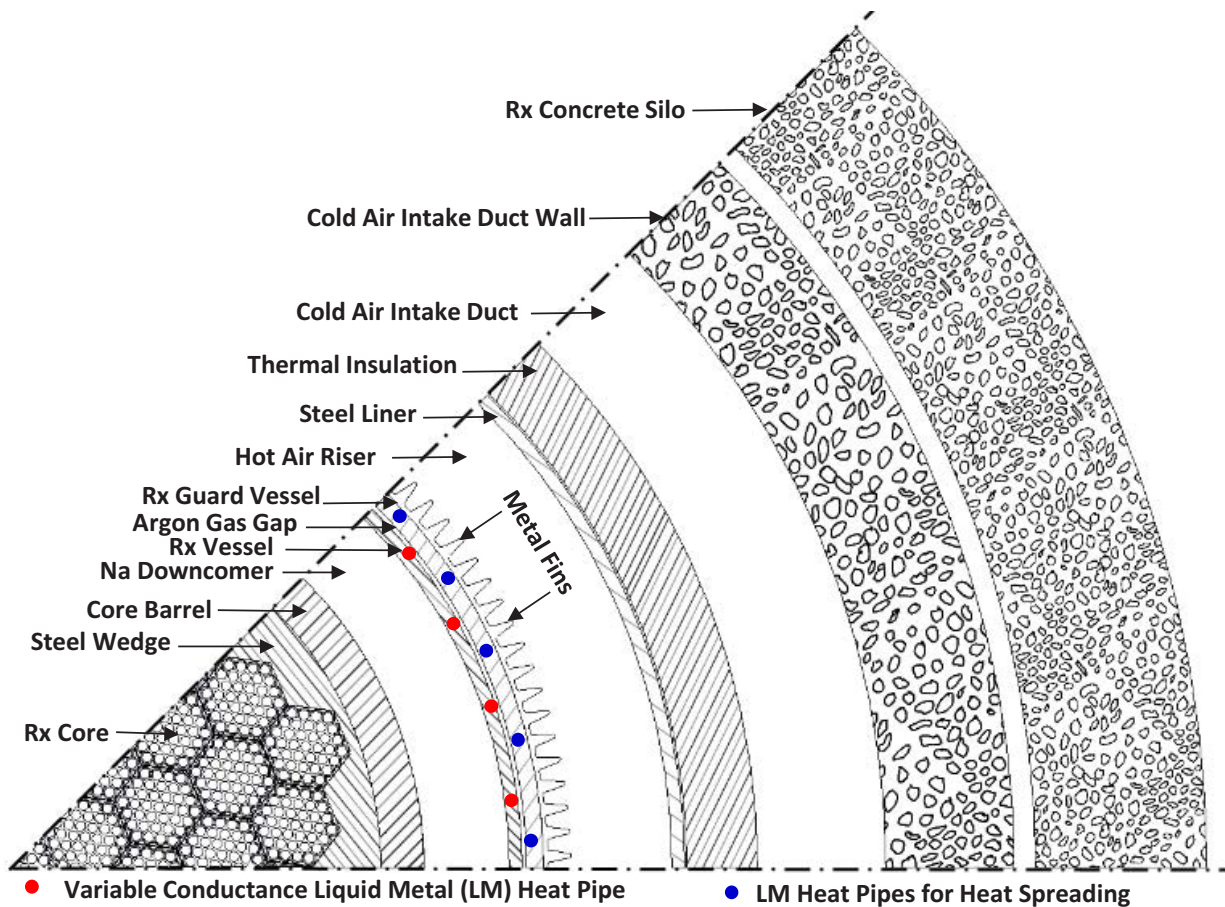


Figure 2. A 30° Cross-Sectional View of the SLIMM Reactor and the Surrounding Structure [1, 3].

The objective of this paper is to quantify the potential of natural circulation of ambient air for removing the decay heat generated in the SLIMM reactor core after shutdown and in case of a malfunction of the in-vessel HEX (Figs. 1 and 3). The performed 3-D Computational Fluid Dynamics (CFD) and thermal-hydraulic analyses calculate the rate of heat removal from the guard vessel outer surface by natural circulation of air and the contribution of thermal radial. In addition, the analyses investigated the effect of

the metal fins on increasing the rate of heat removal from the outer surface of the guard vessel. Also calculated is the change in the average temperature of the in-vessel liquid sodium with time after reactor shutdown, while removing the decay heat by natural circulation of air. The obtained results are for nominal reactor thermal power of $100 \text{ MW}_{\text{th}}$ before shutdown, an in-vessel chimney height of 8 m and an in vessel HEX height of 7 m. (Figs. 1 and 3).

2. METHOD AND APPROACH

The performed 3D-CFD and thermal-hydraulics analyses of ambient air natural convection and thermal radiation along the outer surface of the reactor guard vessel wall used the commercial code package STAR-CCM+, version 10.02 [9]. The analyses investigate the potential of removing the decay heat from the SLIMM reactor after shutdown, in the case of a malfunction of the in-vessel Na/Na HEX (Figs. 2, 3), using natural circulation of ambient air. The natural circulation of the in-vessel liquid sodium removes the decay heat generating in the core, after reactor shutdown, and transport it to the downcomer of the primary vessel. In the downcomer, heat is removed from the circulating liquid sodium by convection to the primary vessel wall. This wall serves as the heat sink for maintaining natural circulation of the in-vessel liquid sodium. As the rate of decay heat generation in the core decreases with time after shutdown, so do the rate of circulation and the average temperature of the in-vessel liquid sodium, including the downcomer.

Immediately after shutdown, the rate of decay heat generation in the core is higher than that removed from the outer surface of the guard vessel by natural circulation of ambient air. The difference will be stored in the in-vessel liquid sodium raising its average temperature. This continues until the rate of decay heat generation drops below that of heat removal by natural circulation of air, causing the average temperature of the in-vessel sodium to peak, then decrease thereafter with increasing time after shutdown.

The present steady-state CFD and thermal-hydraulics analyses, explored the potential of safely removing the decay heat from the SLIMM reactor core by natural circulation of ambient air along the outer surface of the guard vessel wall, with and without metal fins (Figs. 3 and 4). The analyses assume that the temperatures of the circulating liquid sodium the downcomer of the reactor primary vessel are the same as during the reactor nominal operation at $100 \text{ MW}_{\text{th}}$ (core inlet and exit temperatures of 796 K and 610 K, respectively) and changes linearly with distance from the upper plenum (Figs. 1, 3). In reality, these temperatures will temporally increase immediately after shutdown, owing to the malfunction of the in-vessel HEX, before decreasing later in time when the rate of heat removal by ambient air exceeds that of

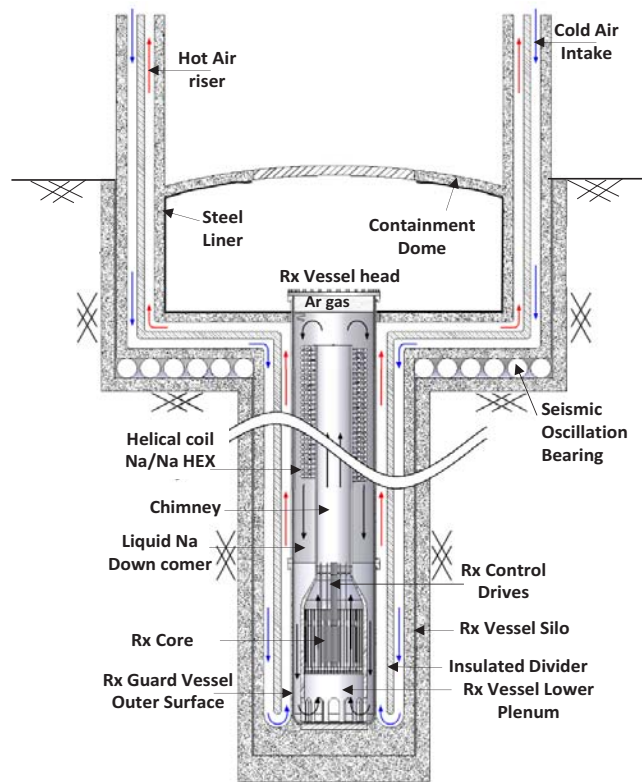


Figure 3. SLIMM Reactor Installed Below Ground and Mounted on Seismic Oscillation Bearings. Natural Circulation of In-Vessel Liquid Sodium Cools the Reactor during Nominal Operation and After Shutdown. In Case of a Malfunction of In-Vessel HEX, Ambient Air Natural Convection, along the Outer Surface of the Guard Vessel Wall, Removes Decay Heat [3].

the decay heat generated in the reactor core by radioactive decay. Therefore, the present steady state estimates of the heat removal by natural circulation by ambient air from the outer surface of the guard vessel would be conservative. Future analyses will consider the transient changes in the temperatures and the circulation rate of the in-vessel liquid sodium with time after reactor shutdown. The present analyses also assume a constant heat transfer coefficient in the reactor downcomer along the inner surface of primary vessel wall. This is reasonable, because of the low Peclet number of the circulating liquid sodium in the downcomer [10].

3. NUMERICAL MESHING

The cold ambient air travels down the intake duct before reversing direction to travel upward in the hot riser (Figs. 3 and 4). It removes the heat dissipated at the outer surface of the guard vessel wall by natural convection and thermal radiation. The difference in the static pressure head between the cold air intake duct and the hot riser drives the air circulation, and hence the rate of the heat removal. Natural convection of air removes the heat dissipated at the surfaces of the guard vessel and metal fins and the steel liner on the facing concrete wall, separating the air intake from the hot riser ducts (Figs. 2-4). Since air is transparent to thermal radiation, the steel liner absorbs the heat emitted from the metal fins by thermal radiation. Subsequently, natural convection to the airflow in the hot riser removes this heat.

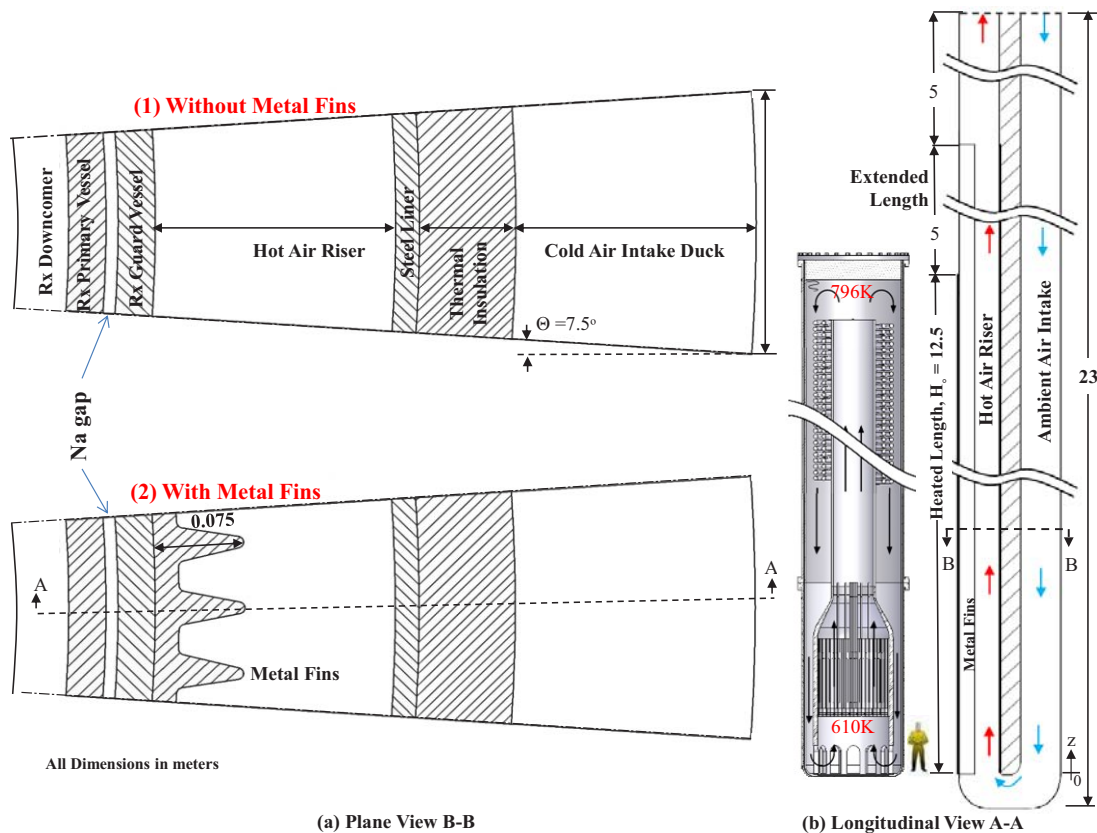


Figure 4. Plane Views and Longitudinal illustration of Decay heat Removal from the Outer Surface of the Guard Vessel Wall, without and with Metal Fins, by Natural Circulation of Air.

For practical consideration to reduce the computational time, the performed analyses used 7.5° pie slice of the SLIMM system (Fig. 4a), with symmetry boundary conditions. For an 8 m tall in-vessel chimney, the height of the reactor vessel wall is 12.5 m, extending to the top surface of the in-vessel liquid sodium (Figs. 1, 3 and 4b). The CFD analyses solve the steady-state conservation equations of mass, momentum

(Navier-Stokes) and energy for the natural circulation of ambient air in the cold intake duct and the hot air riser. They calculate the heat removal rate from the guard vessel wall by air natural convection and by thermal radiation to the steel liner along the opposite wall in the hot air riser.

The CFD analyses use the SST $k-\omega$ turbulence model to simulate the airflow in the cold intake duct and the hot air riser. Wilcox [11] had introduced the original formulation of the $k-\omega$ model, for improving the treatment in the boundary layers, with adverse pressure gradients and separating flows. Menter [12] formulated the SST $k-\omega$ model, by blending a $k-\epsilon$ behavior-like model in the free-stream of the bulk flow with a $k-\omega$ model in the boundary layer near the wall. The combination of the two models

overcomes the solution sensitivity to free-stream conditions. The analyses of the air flow and convection heat transfer use a turbulent Prandtl number, $Pr_t \sim 0.8$ and both the second order upwind convection option and the Durbin Scale limiter realizability scheme for implementing the SST $k-\omega$ model.

In addition to the air flow and the natural convection in the hot riser (Figs. 3 and 4), the analyses estimate the heat transport by thermal radiation from the outer surface of the guard vessel wall, with and without metal fins, to the steel liner on the opposite concrete wall (Figs. 4 and 5). To account for the thermal radiation, the analyses use the gray thermal radiation surface-to-surface model in STAR-CCM+ code package version 10.02 [9], and assume an effective surface emissivity of 0.8. This surface emissivity is achievable by applying a black coating, typically used for space satellites. The convection and radiation heat transfer from the surface of the metal fins along the guard vessel wall is coupled to the 3-D heat conduction in the fins, the walls of the guard and primary vessels and the small Na gap between the vessels (Figs. 2 and 4).

The numerical mesh in the CFD analyses is generated using the STAR-CCM+'s polyhedral mesher, trimmer, the surface re-mesher, and the prism layer mesher. The mesh elements in the solids are polyhedral with an average volume of 134 mm^3 . In the cold airflow in the intake and hot air riser ducts, the numerical mesh is comprised of hexahedral elements (Figs. 5a and 5b). The mesh elements in the hot air riser next to the steel liner and the guard vessel surface, with and without metal fins, are 54 mm^3 in volume, but those in the bulk air flow in the cold intake and the hot riser ducts are larger, 640 mm^3 in volume. In the region of the air flow between the solid surfaces (steel liner and the guard vessel wall or

Table I. Numerical Mesh Elements for the Cases without Metal Fins along the Outer Surface of the Reactor Guard Vessel Wall.

Region		Total Mesh Elements or Cells		
		Coarse	Fine	Finer
Ambient Air	Intake Duck	1,454,313	1,925,710	1,907,756
	Hot Air Riser	4,217,395	21,609,813	23,645,197
Rx Primary Vessel Wall		278,842	609,878	609,880
Liquid Sodium Gap		181,582	339,448	339,448
Rx Guard Vessel Wall		309,667	692,811	692,796
Steel Liner in Hot Riser		126,949	586,308	586,276
TOTAL		6,568,748	25,763,968	27,781,353

Table II. Numerical Mesh Elements for the Cases with Metal Fins along Outer Surface of the Reactor Guard Vessel Wall.

Region		Total Mesh Elements or Cells		
		Coarse	Fine	Finer
Ambient Air	Intake Duck	2,042,216	3,225,692	3,181,423
	Hot Air Riser	10,995,013	50,765,148	53,009,173
Rx Primary Vessel Wall		285,065	609,878	609,880
Liquid Sodium Gap		185,887	339,448	339,448
Rx Guard Vessel Wall		297,695	692,811	692,796
Steel Liner in Hot Riser		118,923	586,308	586,276
Metal Fins		766,460	1,810,832	1,810,816
TOTAL		14,691,259	58,030,117	60,229,812

the metal fins) and the bulk air flow, the numerical mesh grid elements are intermediate is size, 250 mm³ (Figs. 5a and 5b).

To capture the heat transfer by air natural convection and account for the steep temperature drop in the boundaries layer, at the solid surfaces in the hot air riser, the prism-layer meshing tool introduces exponentially refined and parallel prismatic layers in the boundary layers. The present analyses used ten prismatic layers in the 3-mm thick boundary layers. The thickness of the prismatic layers increases with distance from the solid surfaces, by a multiplier of 1.3 (Figs 5a and 5b).

Tables I and II list the number of numerical elements (or cells) used in the solid and airflow regions in three mesh grids (coarse, fine and finer), for the cases without and with metal fins along the outer surface the reactor guard vessel wall (Figs. 4a and 4b). For the case without metal fins, the fine mesh has ~23.6 million fluid elements and ~ 2.2 million solid elements, for 25.8 million elements total (Fig. 5a and Table I). With metal fins (Fig. 5b), the fin grid in Table II consists of ~ 54.0 million fluid elements and ~ 4.04 million solid elements, for a total of ~ 58 million elements (Fig. 5b).

Numerical mesh refinements, listed in Tables I and II, are used to conduct a sensitivity analysis to quantify the effect of the mesh refinement on the calculated results. The results include the rate of heat removal from the outer surface of the guard vessel wall, with and without metal fins, the surface temperature of the steel liner in the hot air riser (Figs. 4 and 5), and the temperature and the velocity distributions and the total flow rate of the air in the hot riser. In addition, the results include the radial temperature distributions in the reactor's primary and guard vessel walls.

Initially, the performed CFD analyses, for the cases without and with metal fins along the guard vessel outer surface, used a coarse mesh comprised of ~ 6.6 and ~14.7 million total elements, with ~5.7 and ~13 million fluid elements, respectively (Tables I and II). Subsequently, the analyses are conducted using both the fine and the finer meshes detailed in Tables II and I. The total elements of the finer mesh, for the cases without and with metal fins, are ~27.8 and ~60.2 million, including ~25.6 and 56.2 million fluid elements, respectively.

Compared to the coarse mesh, the analyses results using the fine mesh, for the cases without and with metal fins, showed ~21.6% and ~ 13.6% increase in the total thermal power removed by the ambient air from the outer surface of the guard vessel wall, respectively, but lower temperatures. The calculated temperatures at the outer surface of the primary and guard vessel walls and at the surface of the metal fins decreased by ~ 0.3% - ~2%, compared to ~ 6% - ~7.9% decrease in the surface temperature of the steel liner in the hot air riser. In addition, the total air flow rate in the hot riser decreased by ~10.4% - ~11.2%, respectively. The CFD analyses results using the finer mesh are almost identical to those using the fine

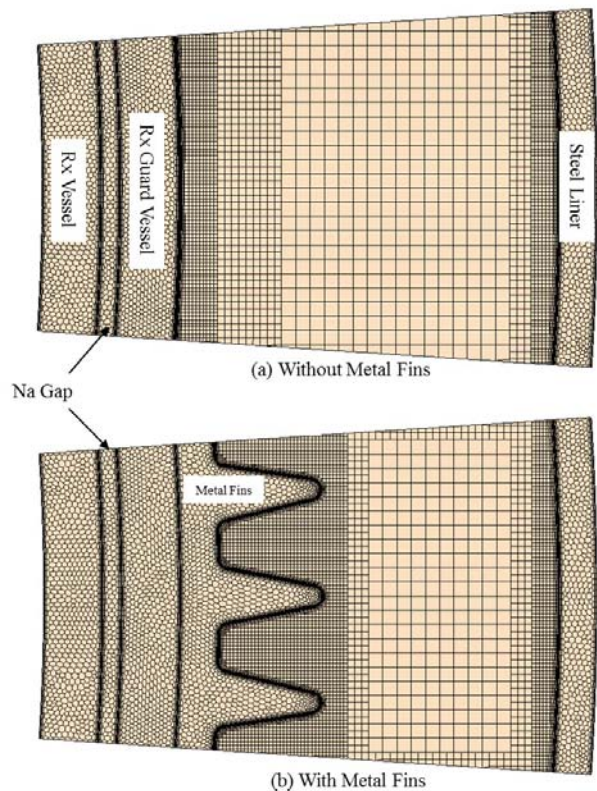


Figure 5. The Fine Numerical Mesh Grids Used in CFD analyses of the Heat Removal by Natural Circulation of Ambient air.

mesh, but required much more time to coverage. Thus, the results presented in the remainder of this paper are calculated using the fine mesh (Tables II and I) for the cases without and with metal fins along the outer surface of the reactor guard vessel wall (Figs. 5a and 5b).

4. RESULTS AND DISCUSSION

Presented in this section are the results of the 3-D, thermal hydraulics and CFD analyses of the decay heat removal from SLIMM by natural convection of ambient air, in case of a malfunction of the in-vessel Na/Na HEX (Figs. 1 – 4). The calculated results are for a reactor nominal thermal power of $100 \text{ MW}_{\text{th}}$ before shutdown and 8-m tall in-vessel chimney (Fig. 1). The performed analyses investigated the effects of using metal fins along the guard vessel and LM heat pipes spreaders on the rate of heat removal by natural convection of ambient air. In addition, the relative contributions of natural convection and thermal radiation to the total rate of heat removal from the outer surface of the guard vessel wall by ambient air are calculated and compared.

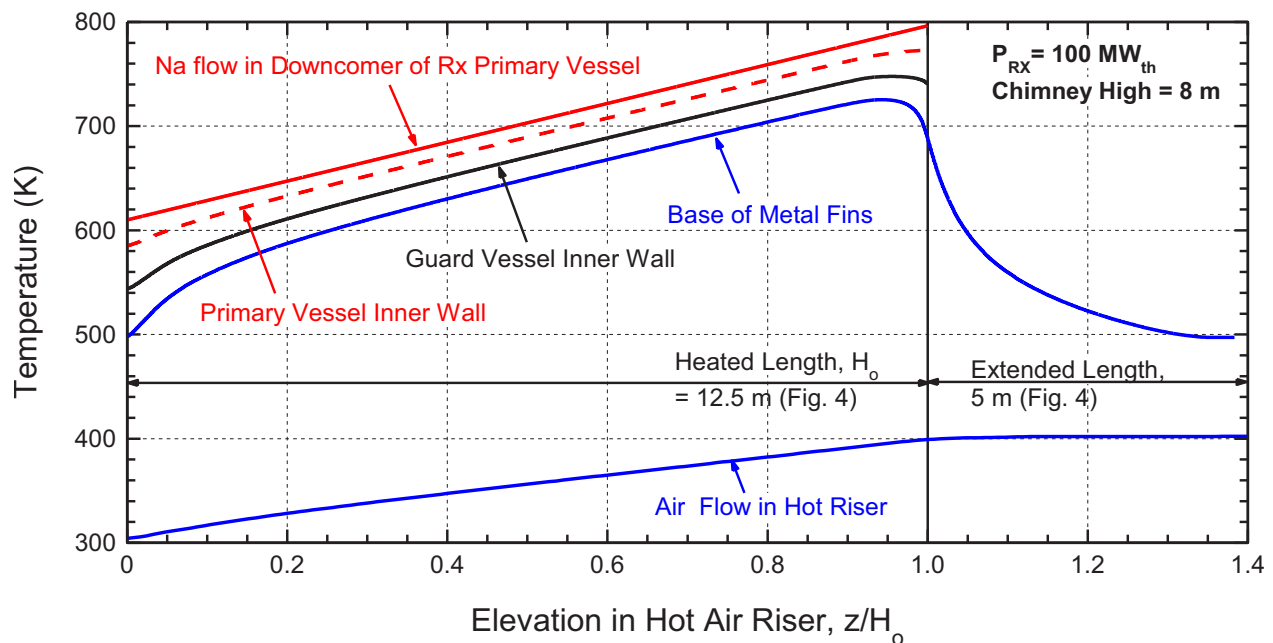


Figure 6. Comparison of the Axial Temperature Distributions Calculated in the Liquid Sodium in the SLIMM Reactor Downcomer, Various Solid Structures and the Hot Riser for the Ambient Air.

4.1. Axial Temperature Distributions

The results presented include the axial temperature distributions in the solid structure and in the airflow in the hot riser (Figs. 3 and 4), and both the radial temperature and velocity profiles in the rising air at different elevation in the hot riser (Fig. 3 and 4). The removed decay heat, from the downcomer of the SLIMM reactor after shutdown, transfers by conduction through the walls of the primary and guard vessels (Figs 4 and 5), the small Na filled gap between the vessels, and the metal fins along the outer surface of the guard vessel. The dissipated heat from the guard vessel wall, without or with metal fins, is removed both by convection to the air in the hot riser and by thermal radiation to the steel liner on the opposite wall (Figs. 2-5). Subsequently, natural convection of air in the hot riser removes the deposited heat in the steel liner by thermal radiation.

Figure 6 compares the calculated axial temperature distributions in the downcomer of the SLIMM reactor primary vessel, along the inner surfaces of the primary and guard vessels walls, at the surface of the metal fins along the guard vessel outer surface (Fig. 4), and of the air bulk temperature in the hot riser (Figs. 3 and 4). These temperatures are plotted versus the axial distance, z , from the entrance of the hot air riser ($z = 0$), normalized to the heated length of the reactor primary vessel wall, H_o . In the performed CFD and thermal-hydraulic analyses, the circulating liquid sodium in the reactor primary vessel enters the downcomer ($z/H_o = 1.0$) at 796 K and exits the lower plenum ($z/H_o = 0.0$) at 610 K [1, 3, 4]. These are the temperatures in the SLIMM reactor with an 8 m tall chimney, during nominal operation at 100 MW_{th} before shutdown. Although these temperatures would change with time after reactor shutdown, they help quantify the highest potential of the backup system for removing the decay heat from the SLIMM reactor primary vessel by natural circulation of ambient air, in case of a malfunction of the in-vessel helically coiled tubes Na/Na HEX (Figs. 1 and 3).

In addition to a negative reactivity feedback, the SLIMM reactor has two independent systems each is capable of scrambling the reactor in case of an emergency (Fig. 1) [1-3]. When the SLIMM shuts down, following a malfunction of the in-vessel HEX, liquid sodium replaces the argon gas in the small gap between the primary and guard vessels, increasing the gap conductance for removing the decay heat from the reactor primary vessel wall. This wall would function as the heat sink for maintaining the natural circulation of the in-vessel liquid sodium, commensurate of the rate of decay heat generation in the reactor core, which decreases with time after reactor shutdown.

The performed 3-D, CFD and thermal-hydraulics analyses account for the changes in the thermal conductivities of the various solid structures and the thermophysical properties of liquid sodium and ambient air with temperature. Since the heat transfer coefficient of the flowing liquid sodium in the downcomer of the SLIMM reactor is constant, due to the low Peclet Number of the flow [10], the temperature drop between the liquid sodium and the inner surface of the reactor primary vessel wall is constant ~ 12 K, regardless of axial elevation ($z/H_o = 0.0-1.0$). The calculated temperature drop for heat conduction in the sodium-filled gap, between the primary and guard vessels, is negligibly small. The temperature drop in the primary vessel wall is ~ 21 K, along most of the heated length, but as much as ~ 30 K near the top of the downcomer ($z = H_o$). Similarly, the temperature drop by conduction in the guard vessel wall to the base of the metal fins (Fig. 4) averages ~ 21 along the heat length, but increases near the top ($z/H_o = 1.0$) and the bottom ($z = 0.0$) of the heated length to as much as ~ 42 K. In the 5-m tall extended length (Fig. 4) of the metal fins ($z/H_o > 1.0$), the LM heat pipes help spread the heat axially in the metal fins. This is indicated by the axial temperature drop at the base of the fins from ~ 700 K at $z/H_o = 1.0$ to ~ 500 K at $z/H_o = 1.4$. The dissipated heat from the extended surface of the metal fins continues to heat the air in the hot riser, but by only a few degrees. To simulate the effect of the LM heat pipes spreaders on axial heat conduction in the metal fins, the analyses assume an axial thermal conductivity that is twice that of solid copper in the radial direction (~ 400 W/m. K). Future work will model in detail the performance of LM heat pipe spreaders [13].

4.2. Radial Temperature Distributions

Figures 7a and 7b present images of the calculated radial temperature fields in the walls of the reactor's primary and guard vessel walls, the Copper fins, and the hot air riser at two axial elevations, $z/H_o = 0.5$ and 0.75 . These images show the heat transfer by natural convection of air from the surfaces of the metal fins and the steel liner, on the opposite wall of the hot air riser (Figs. 2). The dividing wall between the ambient air cold intake and the hot riser is thermally insulated in the cold air duct. Thus, the radial temperature in the steel liner is uniform, but much higher than the bulk temperature of the airflow in the hot riser and lower than that at the surface of the metal fins (Figs. 6 and 7).

Thermal radiation emitted from the metal fins heats the steel liner, cooled by natural convection of air in the hot riser. Because of the higher surface temperature of the metal fins (500 K-720 K, depending on elevation (Fig. 6)), thermal radiation is an important component of dissipating the decay heat from the surface of the metal fins to the steel liner (Figs. 3 and 4). The images in Figs. 7a and 7b also show that the thicknesses of the thermal boundary layers at the surfaces of the metal fins and the steel liner increase with increasing elevation, as the rising air heats up. The temperatures of the solid structure (reactor vessel walls and the metal fins) as well as those of the steel liner and the air in the hot riser increase with increased elevation.

Figure 8 compares the calculated radial temperature distributions, extending from the inner surface of the primary vessel wall ($r/R_v = 0$ where, R_v is the inner radius of the reactor vessel) to the steel liner ($r/R_v = 1.24$), along the dividing concert wall between the cold air intake duct and the hot air riser (Figs. 3 and 4). Figure 8 compares the calculated temperature profiles along the dashed line in the insert, at axial elevations of $z/H_o = 0.5$, 0.75 and 1.0 (end of the directly heated length of the reactor primary vessel) (Fig. 4). These profiles show the steep temperature drops in the boundary layers at the surfaces of the metal fins and the facing steel liner. Note that the radial temperature gradient in the metal base and the metal fins, along the outer surface of the reactor guard vessel, is very small, owing to the Copper higher thermal conductivity.

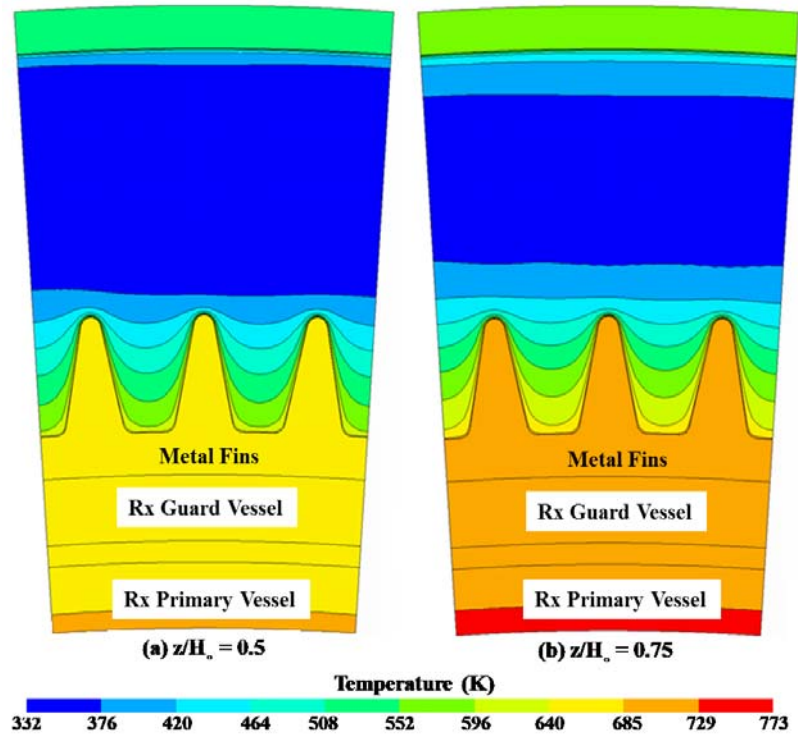


Figure 7. Calculated Temperatures in Reactor Vessels Walls, Metal Fins, and Hot Air Riser.

The calculated temperatures in the solid regions, increase with axial elevation, except at the end of the directly heated length ($z/H_o = 1.0$), it slightly decreases due to the axial conduction into the extended length of the metal fins using LM heat pipes (Figs. 4). In the rising hot air, the temperatures in the radial distribution also increase with axial elevation. The hot riser, the air temperature is highest at the surface of the metal fins and about 200 K lower, but still high (> 500 K), at the surface of the steel liner. The air temperature decreases almost exponentially with radial distance from either the metal fins or the steel liner, to the lowest values near the surface of the metal fins (Fig. 8).

4.3. Radial Velocity Profiles in Hot Air Riser

Figure 9 compares the calculated radial velocity profiles in the airflow in the hot riser (Fig. 4), along the reactor guard vessel, at different axial elevations of $z/H_o = 0.5$, 0.75 and 1.0. The hot air velocities increase with increasing axial elevation. This is because the increase in air temperature decreases its density and viscosity and, hence, increases the radial velocity profile. In the radial velocity distributions in the annular duct of the hot riser (Fig. 4), the air maximum velocity moves away from the surface of the

metal fins with axial elevation (Fig. 9). This is because the temperature of the rising air near the metal fins is higher than that near the steel liner on the opposite wall (Figs. 7 and 8). The air velocity at the surfaces of the metal fins and the steel liner is zero, because of the non-slip condition at the air-solid interfaces. The peak air velocity in the hot riser (Fig. 4) is ~ 8.423 m/s at $z/H_0 = 0.5$, and ~ 9.2 and ~ 10 m/s at $z/H_0 = 0.75$ and 1.0 , respectively. These peak velocities occur at a radial distance, $r/R_v = 1.148$, 1.156 and 1.156 , respectively (Fig. 9).

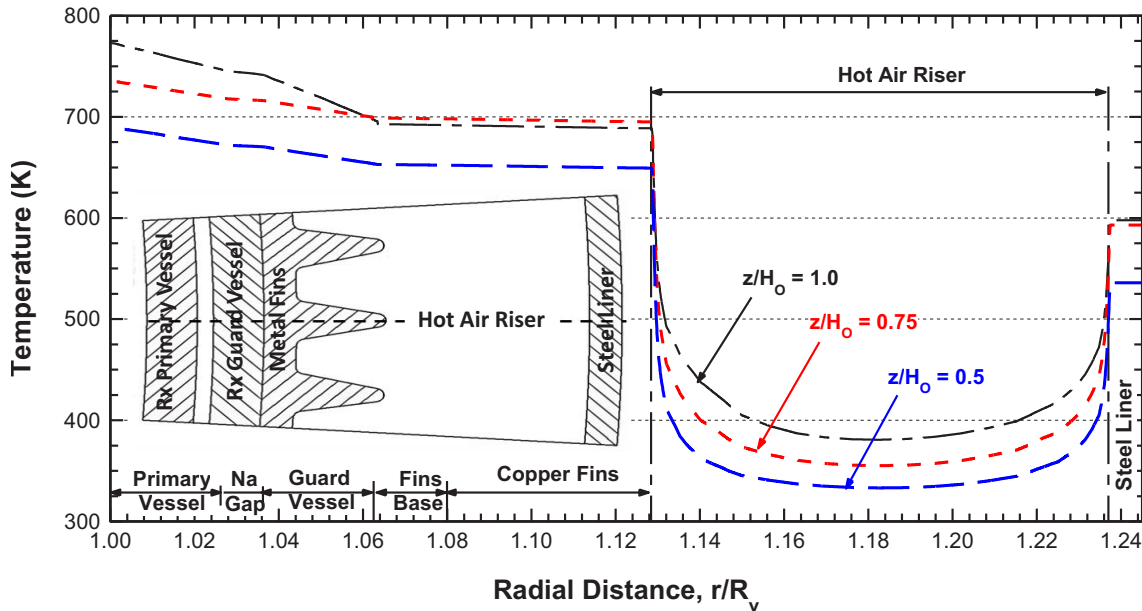


Figure 8. Calculated Radial Temperature Profiles at Different Elevations in the Hot Air Riser.

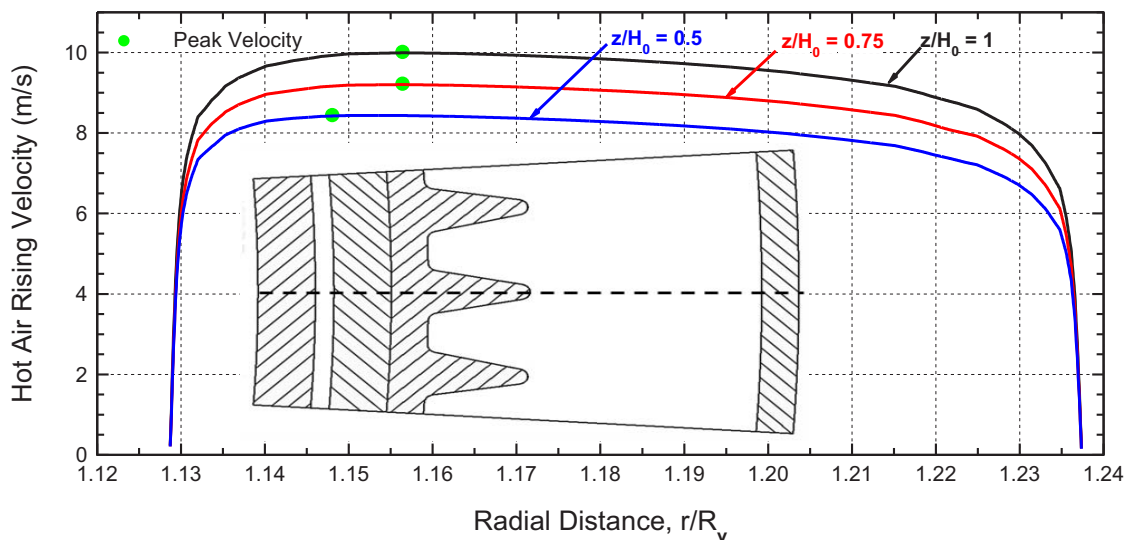


Figure 9. Comparison of Calculated Radial Velocity Profiles of Ambient Air in the Hot Riser.

5. DECAY HEAT REMOVAL

The performed 3-D thermal-hydraulics and CFD analyses investigated the effects of: (a) having metal fins along the outer surface of the guard vessel wall, (b) extending the length of the metal fins beyond the

heated length of the reactor primary vessel wall, and (c) using LM heat pipes heat spreaders, on the heat removal capability by ambient air. The rate of the decay heat removal by ambient air depends on the temperature of the circulating liquid sodium in the downcomer of the reactor primary vessel, which depends on the height of the in-vessel chimney (Fig. 3) and the reactor thermal power before shutdown. These temperatures decrease with time after reactor shutdown, hence decreasing the heat removal rate by the natural circulation of ambient air.

Results presented graphically in Figs.10a show that, without metal fins, the total heat removed by ambient air natural circulation is $\sim 1.0 \text{ MW}_{\text{th}}$ (Fig. 10a), or which 58% is removed by natural convection of air (Figs. 3 and 4), and 42% by thermal radiation to the steel liner. Because air is transparent, the heat transported by thermal radiation to the steel liner is removed by natural convection of air. Adding metal fins along the outer surface of the guard vessel wall, but of the same height as that of the heated vessel wall (Figs. 4 and 10b), increases the total heat removed by ambient air by 26% to $1.26 \text{ MW}_{\text{th}}$. However, the contribution to the total heat removal by natural convection increases to 70%, while that by thermal radiation decreases to 30%.

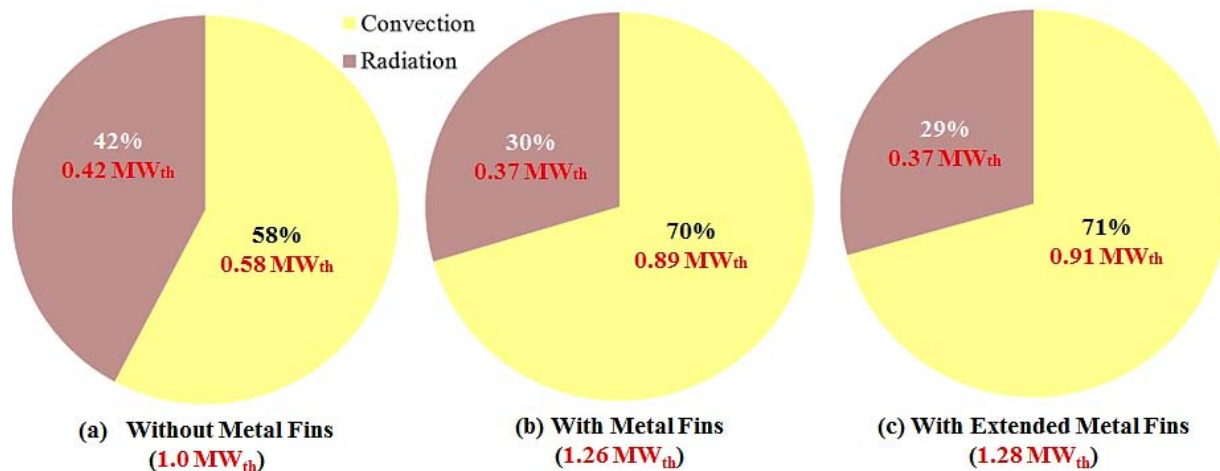


Figure 10. Estimates of Decay Heat Removal by Natural Circulation of Ambient Air.

Extending the metal fins by an additional 5 m, beyond that of the heated vessel wall (12.5 m), and using LM heat pipes along the base of the metal fins (Fig. 4), increase the total heat removed by natural circulation of ambient by only 1.6% to $1.28 \text{ MW}_{\text{th}}$ (Fig. 10c). The contribution of the air natural convection at the surface of metal fins increases to 71%, while that of the thermal radiation decreases to 29%. These estimates assume that the LM heat pipes increase the effective axial conductivity to 800 W/m K , twice that of the Copper fins, which is a conservative assumption [13].

The estimates in Figs. 10a and 10b of the rate of decay heat removal by natural circulation of ambient air from the SLIMM reactor after shutdown, in case of a malfunction of the in-vessel HEX, are used to estimate the average temperature of the In-vessel liquid sodium as a function time after shutdown (Fig. 11). For the SLIMM reactor with 8 m tall chimney, the total mass of the in-vessel liquid sodium is $\sim 38 \text{ MT}$ [1, 3]. Initially, the rate of decay heat generation is higher than that of the heat removal by the ambient air from the surface of the reactor guard vessel, causing the average temperature of the in-vessel liquid sodium to increase temporarily. This temperature peaks, when the rate of decay heat removal equals that of heat removal. Beyond such time, the decay heat generation rate drops below that of the heat removal by natural convection of ambient air, causing the temperature of the in-vessel liquid sodium to decrease progressively with time (Fig. 11).

Figure 11 compares the estimates of the average temperature of the in-vessel sodium after reactor shutdown for two cases: (a) No metal fins at the outer surface of the reactor guard vessel, and (b) there are metal fins along the heated wall of the reactor guard vessel. In both cases, the total rate of heat removal by natural convection and thermal radiation from the guard vessel, with and without metal fins, is 1.0 and 1.26 MW_{th}, respectively (Figs. 10a and 10b). Without metal fins, the average temperature of the liquid sodium in the primary vessel (Figs. 3 and 4) peaks at ~ 821.7 K, ~ 1.5 hr after reactor shutdown and decreases to 400 K (slightly higher than the sodium melting temperature of 371 K) ~ 22.2 hr after reactor shutdown. With metal fins, the rate of heat removal by ambient air increases by 26% to 1.26 MW_{th} (Fig. 10b). Such higher rate limits the peak temperature of the in-vessel liquid sodium to ~ 806 K, only ~ 40 minutes (or 0.665 hr) after reactor shutdown. In addition, the in-vessel liquid sodium cools down to 400 K, ~ only 13.5 hr after shutdown (Fig. 11).

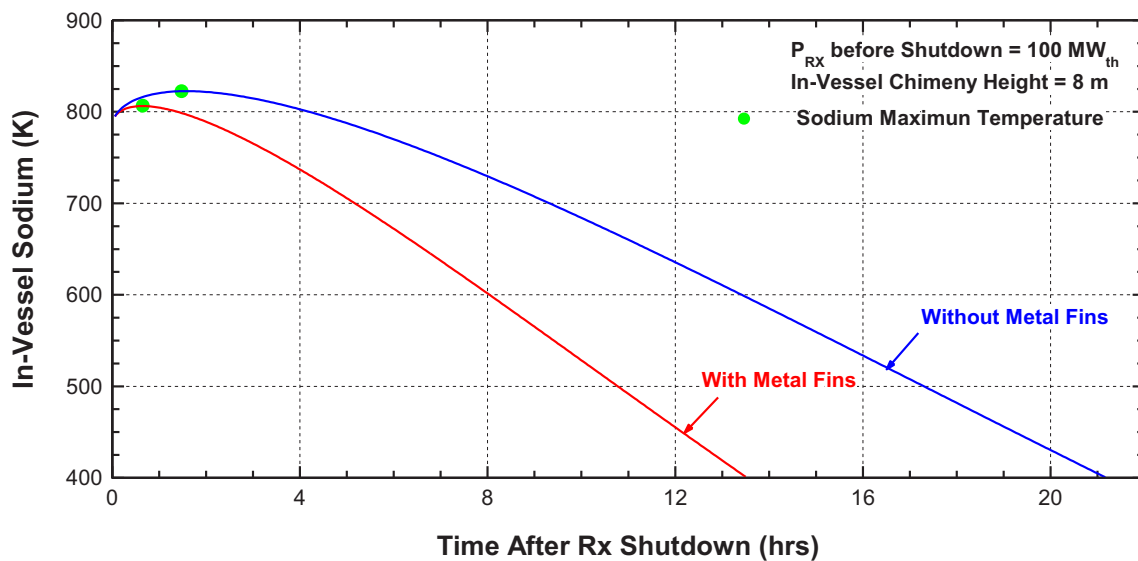


Figure 11. In-Vessel Liquid Sodium Temperature with Decay Heat Removal by Ambient Air.

4. SUMMARY AND CONCLUSION

The SLIMM reactor developed at the University of New Mexico’s Institute for Space and Nuclear Power Studies can generate 10 – 100 MW_{th} for extended periods, while cooled by natural circulation of in-vessel liquid sodium, with the aid of a tall chimney and a helically coiled tubes Na/Na heat exchanger (HEX). The HEX, placed at the top of the downcomer, maximizes the driving static pressure for cooling the reactor core by natural circulation during full power operation and after shutdown. In the unlikely event of a malfunction of the in-vessel heat exchanger, the reactor shuts down, and natural circulation of ambient air, along the outer surface of the guard vessel wall, passively removes the decay heat generating in the reactor core. This work performed 3-D thermal-hydraulics and CFD analyses to quantify the potential of natural convection of ambient air for removing the decay heat after reactor shutdown.

Results showed that the decay heat removal by ambient air is quite effective, even without metal fins along the outer surface of the guard vessel. Nonetheless, the metal fins increase the rate of the heat removal by naturally convection of ambient air, by an additional 26% to 1.26 MW_{th}. Without metal fins along the guard vessel outer surface, the average temperature of the circulating liquid sodium in the reactor primary vessel peaks at ~ 821.7 K, ~ 1.5 hr after reactor shutdown and decreases to 400 K ~ 22.2 hr after reactor shutdown. With metal fins, the higher rate of heat removal (1.26 MW_{th}), limits the peak temperature of the in-vessel liquid sodium to ~ 806 K, only ~ 40 minutes (or 0.665 hr) after reactor

shutdown. These results confirm a large safety margin of > 330 K from the boiling temperature of liquid sodium (~ 1156 K at 0.1 MPa).

REFERENCES

1. M. S. El-Genk and L. M. Palomino, "SLIMM-Scalable Liquid Metal Cooled Small Modular Reactor," *Proceedings of ICAPP 2014*, Paper #14076, Charlotte, NC, USA, April 6-9 (2014).
2. M. S. El-Genk and L. M. Palomino, "SLIMM -Neutronic Analyses and Lifetime Estimates," *Proceedings of ICAPP 2014*, Paper #14232, Charlotte, NC, USA, April 6-9 (2014).
3. M. S. El-Genk and L. M. Palomino, "SLIMM-Scalable Liquid Metal Cooled Small Modular Reactor: Preliminary Design and Performance Analyses," *J. Progress in Nuclear Energy* (in print, 2015).
4. D. A. Haskins and M. S. El-Genk, "Natural Circulation Model and Performance Analyses of "SLIMM"- A Small, Modular Sodium-Cooled Reactor," *Proceeding NURETH-16*, Paper #13514, Chicago, IL, (3 August - 4 September 2015).
5. R. P. Anantamula and W. F. Berhm, W. F., *Sodium Compatibility of HT-9 and Fe-9Cr-1Mo Steels*, Technical Report HEDL-SA-2801FP, Westinghouse Hanford Company. (1985).
6. R. I. Klueh and D. J. Alexander, "Heat Treatment Effects on Impact Toughness of 9Cr-1MoVNb and 12Cr-1MoVW Steels Irradiated to 100 dpa," *J. Nuclear Materials*, **253-258**, 1269-1274 (1998).
7. S. A. Maloy, M. B. Toloczko, J. Cole and T. S. Byun, "Core Materials Development for the Fuel Cycle R&D Program" *J. Nuclear Materials*, **415**, pp. 302 (2011).
8. O. J. Foust, *Sodium-NaK Handbook, Vol. I*, Gordon and Breach, New York, USA (1972).
9. CD-adapco, STAR-CCM+ Release 10.02, <http://www.cd-adapco.com/> (2014)
10. T. M. Schriener and M.S. El-Genk, "Convection Heat Transfer of NaK-78 Liquid Metal in a Circular Tube and a Tri-lobe Channel," *Int. J. Heat and Mass Transfer*, **86**, 234 – 243 (2015).
11. D. C. Wilcox, "Turbulence Modeling for CDF," 2nd Edition, DCW Industries, Inc. (1998).
12. F. R. Menter, "Two-equation eddy-viscosity turbulence modeling for engineering applications," *AIAA Journal*, **32**, 1598-1605 (1994).
13. M. S. El-Genk and J.-M. P. Tournier, "Uses of Liquid-Metal and Water Heat Pipes in Space Reactor Power Systems," *J. Frontiers in Heat Pipes*, **2**(1), 3002 (2011).